

Bright filter-free source of indistinguishable photon pairs

F. Wolfgramm,¹ X. Xing,² A. Cerè,¹ A. Predojević,¹ A. M. Steinberg,²
and M. W. Mitchell¹

¹*ICFO - Institut de Ciències Fotoniques, Mediterranean Technology Park,
08860 Castelldefels (Barcelona), Spain*

²*Centre for Quantum Information & Quantum Control and Institute for Optical Sciences,
Dept. of Physics, 60 St. George St., University of Toronto, Toronto, ON, Canada, M5S 1A7*

florian.wolfgramm@icfo.es

Abstract: We demonstrate a high-brightness source of pairs of indistinguishable photons based on a type-II phase-matched doubly-resonant optical parametric oscillator operated far below threshold. The cavity-enhanced down-conversion output of a PPKTP crystal is coupled into two single-mode fibers with a mode coupling efficiency of 58%. The high degree of indistinguishability between the photons of a pair is demonstrated by a Hong-Ou-Mandel interference visibility of higher than 90% without any filtering at an instantaneous coincidence rate of 450 000 pairs/s per mW of pump power per nm of down-conversion bandwidth. For the degenerate spectral mode with a linewidth of 7 MHz at 795 nm a rate of 70 pairs/(s mW MHz) is estimated, increasing the spectral brightness for indistinguishable photons by two orders of magnitude compared to similar previous sources.

© 2021 Optical Society of America

OCIS codes: (270.0270) Quantum optics; (190.4410) Nonlinear Optics, parametric processes; (230.6080) Sources.

References and links

1. Z. Y. Ou and L. Mandel, "Violation of Bell's inequality and classical probability in a two-photon correlation experiment," *Phys. Rev. Lett.* **61**, 50–53 (1988).
2. E. Knill, R. Laflamme, and G. J. Milburn, "A scheme for efficient quantum computation with linear optics," *Nature (London)* **409**, 46–52 (2001).
3. M. W. Mitchell, J. S. Lundeen, and A. M. Steinberg, "Super-resolving phase measurements with a multiphoton entangled state," *Nature (London)* **429**, 161–164 (2004).
4. P. G. Kwiat, K. Mattle, H. Weinfurter, A. Zeilinger, A. V. Sergienko, and Y. Shih, "New high-intensity source of polarization-entangled photon pairs," *Phys. Rev. Lett.* **75**, 4337–4341 (1995).
5. Although we express the efficiency as pairs/(s mW nm) or pairs/(s mW MHz) for comparison with previous sources and in preparation for future experiments with atoms, in this experiment the pump power is not a limiting factor.
6. A. Fedrizzi, T. Herbst, A. Poppe, T. Jennewein, and A. Zeilinger, "A wavelength-tunable fiber-coupled source of narrowband entangled photons," *Opt. Express* **15**, 15377–15386 (2007).
7. O. Kuzucu and F. N. C. Wong, "Pulsed Sagnac source of narrow-band polarization-entangled photons," *Phys. Rev. A* **77**, 032314 (2008).
8. Z. Y. Ou and Y. J. Lu, "Optical parametric oscillator far below threshold: Experiment versus theory," *Phys. Rev. Lett.* **83**, 2556–2559 (2000).
9. Y. J. Lu, R. L. Campbell, and Z. Y. Ou, "Mode-locked two-photon states," *Phys. Rev. Lett.* **91**, 163602 (2003).
10. H. Wang, T. Horikiri, and T. Kobayashi, "Polarization-entangled mode-locked photons from cavity-enhanced spontaneous parametric down-conversion," *Phys. Rev. A* **70**, 043804 (2004).

11. C. E. Kuklewicz, F. N. C. Wong, and J. H. Shapiro, "Time-bin-modulated biphotons from cavity-enhanced down-conversion," *Phys. Rev. Lett.* **97**, 223601 (2006).
 12. J. S. Neergaard-Nielsen, B. M. Nielsen, H. Takahashi, A. I. Vistnes, and E. S. Polzik, "High purity bright single photon source," *Opt. Express* **15**, 7940–7949 (2007).
 13. M. Scholz, F. Wolfgramm, U. Herzog, and O. Benson, "Narrow-band single photons from a single-resonant optical parametric oscillator far below threshold," *Appl. Phys. Lett.* **91**, 191104 (2007).
 14. C. K. Hong, Z. Y. Ou, and L. Mandel, "Measurement of subpicosecond time intervals between two photons by interference," *Phys. Rev. Lett.* **59**, 2044–2046 (1987).
 15. R. B. A. Adamson, L. K. Shalm, M. W. Mitchell, and A. M. Steinberg, "Multiparticle state tomography: Hidden differences," *Phys. Rev. Lett.* **98**, 043601 (2007).
 16. D. J. Heinzen, J. J. Childs, J. E. Thomas, and M. S. Feld, "Enhanced and inhibited visible spontaneous emission by atoms in a confocal resonator," *Phys. Rev. Lett.* **58**, 1320–1323 (1987).
 17. F. De Martini, G. Innocenti, G. R. Jacobovitz, and P. Mataloni, "Anomalous spontaneous emission time in a microscopic optical cavity," *Phys. Rev. Lett.* **59**, 2955–2958 (1987).
 18. A. Kuhn, M. Hennrich, and G. Rempe, "Deterministic single-photon source for distributed quantum networking," *Phys. Rev. Lett.* **89**, 067901 (2002).
 19. G. D. Boyd and D. A. Kleinman, "Parametric interaction of focused gaussian light beams," *J. Appl. Phys.* **39**, 3597–3641 (1968).
 20. R. Le Targat, J.-J. Zondy, and P. Lemonde, "75%-Efficiency blue generation from an intracavity PPKTP frequency doubler," *Opt. Commun.* **247**, 471–481 (2005).
 21. B. Boulanger, M. M. Fejer, R. Blachman, and P. F. Bordui, "Study of KTiOPO₄ gray-tracking at 1064, 532, and 355 nm," *Appl. Phys. Lett.* **65**, 2401–2403 (1994).
 22. W. P. Grice and I. A. Walmsley, "Spectral information and distinguishability in type-II down-conversion with a broadband pump," *Phys. Rev. A* **56**, 1627–1634 (1997).
 23. A. Fedrizzi, T. Herbst, M. Aspelmeyer, M. Barbieri, T. Jennewein, and A. Zeilinger, "Detection of hidden entanglement by photon anti-bunching", arXiv:quant-ph/0807.4437v1 (2008).
 24. Z. Y. Ou and L. Mandel, "Further evidence of nonclassical behavior in optical interference," *Phys. Rev. Lett.* **62**, 2941–2944 (1989).
-

1. Introduction

Indistinguishable photons exhibit non-classical interference, the basis for applications including entanglement generation [1], linear-optics quantum computing [2], and super-resolving phase measurements [3]. Many down-conversion sources [4, 6, 7] achieve indistinguishability by spectral and/or spatial filtering, at the cost of reduced efficiency. In contrast, cavity-enhanced down-conversion [8, 9, 10, 11, 12, 13] promises to produce photon pairs with cavity-defined, and thus controllable, spatial and spectral characteristics. In this spirit, Ou *et al.* [8] used a type-I optical parametric oscillator (OPO) far below threshold to produce a two-photon state that was later shown to be mode-locked and consisting of indistinguishable photons by observing the Hong-Ou-Mandel effect with moderate visibility [9, 14]. A high-purity source of heralded single photons was recently demonstrated by Neergaard-Nielsen *et al.* [12] with a sub-threshold type-I OPO and filters to select heralding photons from a single mode. Kuklewicz *et al.* [11] used a type-II OPO below threshold with temporal filtering (selection of nearly-coincident pairs), to demonstrate a high-brightness source with up to 76.8% Hong-Ou-Mandel interference visibility. The source that we demonstrate here avoids filtering altogether: all output of the source is used, giving a brightness tens to hundreds of times higher than earlier sources. At the same time, high-quality pairs are produced, as demonstrated by a high-visibility Hong-Ou-Mandel dip. The source is also tunable to a rubidium resonance, allowing studies of light-atom interactions with photon pairs.

Despite energy conservation and phase-matching requirements, parametric down-conversion is generally under-constrained, allowing emission into a range of energy and momentum states. Emitted photons are correlated in energy and momentum, providing both an entanglement resource and a challenge to efficient collection. By their nature, position-momentum entangled states cannot be efficiently collected into single-mode optics. Correlations between observed and unobserved variables can also render the photons distinguishable and destroy quantum

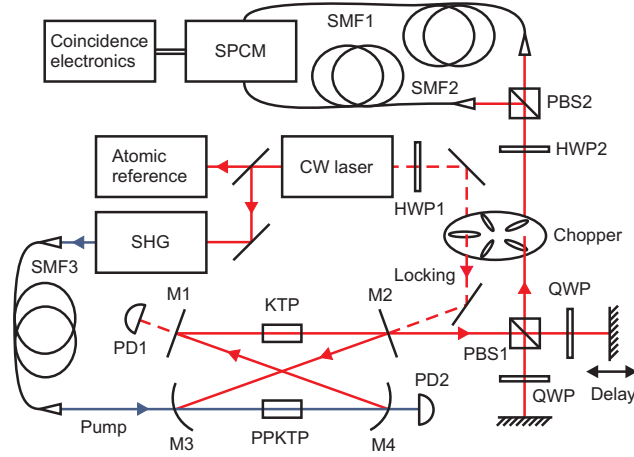


Fig. 1. Experimental Setup. PPKTP, phase-matched nonlinear crystal; KTP, compensating crystal; M1-4, cavity mirrors; PBS, polarizing beam splitter; HWP, half wave plate; QWP, quarter wave plate; SMF, single-mode fiber; PD, photodiode

interference [15]. While filters can "erase" the distinguishing information, they change the nature of the source, from one which produces entangled pairs (and nothing else) to one which sometimes produces unpaired photons. Also, the heralding efficiency is reduced, exponentially decreasing the success probability in a multi-photon heralded experiment. Rather than use filters, we place the down-conversion within a resonant cavity [8, 11]. As with other spontaneous processes [16, 17, 18], this constrains the emission to the cavity modes and enhances the emission rate into those modes. The cavity is designed and stabilized for simultaneous resonance on all longitudinal modes within the phase-matching bandwidth, producing both a very bright source and pair indistinguishability.

2. Experimental setup

As laser source we use a frequency-doubled diode laser system (Toptica TA-SHG 110). The laser wavelength is stabilized to the D_1 transition of atomic rubidium at 795 nm and then frequency doubled to generate the 397.5 nm pump that is passed through a mode-cleaning single-mode fiber and is focused into the center of a 20 mm-long periodically-poled KTiOPO_4 (PPKTP) crystal in a cavity, forming the OPO (Fig. 1). A pump beam waist of 30 μm is achieved with a telescope. This beam waist was chosen to be larger than the optimum for degenerate down-conversion according to Boyd and Kleinman [19] in order to reduce possible effects of thermal lensing [20] and gray-tracking [21]. The crystal is poled for type-II degenerate down-conversion, and produces orthogonally-polarized signal and idler photons. Due to crystal birefringence, these photons experience temporal walk-off which would, if un-compensated, render the photons temporally distinguishable. A second KTP crystal of the same length and crystal cut, but not phase-matched and rotated about the beam direction by 90° , is added to the long arm of the cavity in order to introduce a second walk-off equal in magnitude but opposite in sign [11].

The ring cavity is formed by two flat mirrors (M1, M2) and two concave mirrors (M3, M4) with a radius of curvature of 100 mm. The effective cavity length of 610 mm corresponds to a free spectral range (FSR) of 490 MHz. This geometry provides a beam waist of 42 μm for the resonant down-converted beam at the center of the crystal, which matches the 30 μm pump beam waist. Cavity length is controlled by a piezoelectric transducer on mirror M1. The output

coupler M2 has a reflectivity of 93% at 795 nm. All other cavity mirrors are highly reflecting ($R > 99.9\%$) at 795 nm and highly transmitting at 397.5 nm ($R < 3\%$) resulting in a single-pass through the nonlinear crystal for the blue pump beam. The crystal endfaces are AR coated for 397.5 nm and 795 nm. The measured cavity finesse of 70 results in a cavity linewidth of 7 MHz.

While the walk-off per round trip is compensated by the KTP crystal, there is an uncompensated walk-off of in average half a crystal-length, because of the different positions inside the PPKTP, where a photon pair could be generated. This leads to a remaining temporal distinguishability at the output of the cavity that is completely removed by delaying the horizontally polarized photon of each pair with a Michelson-geometry compensator: a polarizing beam splitter, retro-reflecting mirrors, and quarter wave-plates set to 45° introduce an adjustable delay while preserving spatial mode overlap. After recombination the pairs are sent through a half wave plate (HWP2) that together with PBS2 determines the measurement basis. Both output ports of PBS2 are coupled into single-mode fibers (SMF) connected to single photon counting modules (Perkin Elmer SPCM-AQ4C). The pulse events are registered and processed by coincidence electronics (FAST ComTec P7888) with a resolution of 1 ns.

The OPO cavity is actively stabilized by injecting an auxiliary beam, derived from the diode laser, into the cavity via the output coupler (M2). This light is detected in transmission by a photodiode (PD1). Frequency modulation at 20 MHz is used to lock to the peak of the cavity transmission. To eliminate the background noise caused by this auxiliary beam and to protect the SPCMs, the locking and measuring intervals are alternated using a mechanical chopper at a frequency of about 80 Hz with a duty cycle of 24%.

To achieve degeneracy of the H/V modes, we set the polarization of the auxiliary beam to 45° and measure the cavity transmission for H- and V-polarized components. The transmission peaks for the two polarizations are overlapped by temperature tuning of the compensating KTP crystal, whereas the temperature of the PPKTP crystal is kept stable at the optimal phase-matching temperature for degenerate operation at 42.0°C . Both crystals are temperature controlled with a long-term stability of better than 5 mK corresponding to an overlap between the transmission spectra for H- and V-polarized components of better than 95%.

The pump power after the cavity is measured by collecting a constant fraction on a photodiode (PD2). This system is calibrated against the total power passing through the PPKTP crystal as measured by a power meter (Coherent FieldMate). Over the duration of any given measurement, the power was stable to within 5%. We used a typical optical pump power of 200 μW to reduce the probability of generation of two pairs within the cavity ring-down time. The optimization of the pump beam mode-matching was performed by maximizing the count rates on the single-photon detectors.

3. Arrival-time correlation measurement

Without correcting for any losses, the photon rate in each arm ($R_{\text{SMF1,SMF2}}$) was measured to be 142 000 counts/s during the measurement period (when the chopper was open) with a coincidence rate of 34 000 pairs/s. The unavoidable accidental coincidence rate R_{acc} in the coincidence time window of $\tau = 256$ ns is calculated by $R_{\text{acc}} = R_{\text{SMF1}} R_{\text{SMF2}} \tau = 5\,000$ pairs/s, resulting in a corrected coincidence rate of 29 000 pairs/s, that is, a collection efficiency of 20%. The FWHM of the crystal phase-matching bandwidth is calculated by $1/(|k'_s - k'_i|L) = 148$ GHz, with the crystal length L and the k -vectors for signal and idler photons [23]. Considering this bandwidth a spectral brightness of 450 000 pairs/(s mW nm) [5] is calculated, brighter by a factor of 1.6 compared to the single-pass SPDC source in [6] with a coincidence rate of 273 000 pairs/(s mW nm).

Within the crystal bandwidth the output spectrum consists of roughly 600 modes, the degenerate one at the rubidium D_1 line. The modes are spaced by a FSR of 490 MHz, each of them

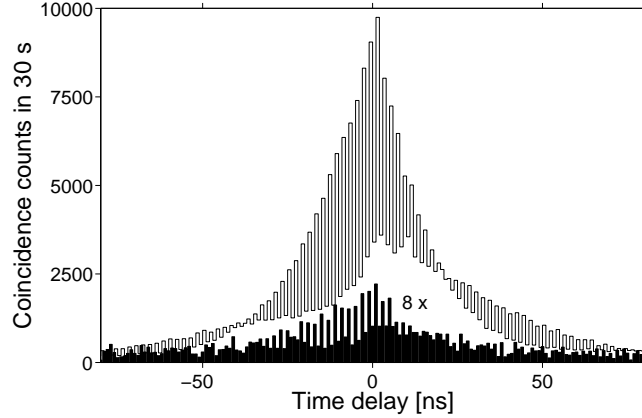


Fig. 2. Histogram of difference between signal and idler arrival times in the $\pm 45^\circ$ basis (multiplied by 8, lower curve) and in the H/V basis (upper curve) without path difference between signal and idler beam paths

having a bandwidth of 7 MHz. For the degenerate mode, which contains about 1/300 of the total output, the photon coincidence rate is estimated to be 70 pairs/(s mW MHz), two orders of magnitude higher than the rate of 0.7 pairs/(s mW MHz) reported in [11].

Taking into account the limited quantum efficiency of the detectors (49%), the single-mode fiber coupling efficiency (58%), the escape efficiency of the cavity (82%) and the overall transmission through all optical elements after the cavity (90%) a conditional detection efficiency of 21% is expected. The fact that the measured efficiency agrees with this expectation proves that the emission from the cavity itself is in a single spatial mode. Given this parameter, we estimate the true pair production rate to be 3.4×10^6 pairs/(s mW).

We measured the arrival time difference between detection events on the two SPCMs in a time window of 256 ns over 30 seconds in the H/V and $\pm 45^\circ$ bases (Fig. 2). The time correlation graph shows the typical double-exponential decay reflecting the ring-down time of the cavity. The time delay between the photons of a pair is always an integer multiple of the round trip time, resulting in the comb structure of Fig. 2, in which alternating bins have low and high count rates. The contrast of this oscillation is modulated due to the sampling resolution of 1.0 ns and the 2.03 ns round trip time, vanishing every 31 peaks as can be seen in Fig. 2. These results agree with the theory given in [11] for the case of compensated birefringence.

4. Hong-Ou-Mandel measurement

When the relative delay between the two photons of a pair is changed, their degree of temporal indistinguishability is varied and the Hong-Ou-Mandel effect [14] can be observed. When we measure in the $\pm 45^\circ$ basis and with no delay, signal and idler photons of a pair impinging on PBS2 are indistinguishable and exit on the same output port of PBS2 leading to a drop in the coincidence rate as shown in Fig. 2.

The coincidence rate in the $\pm 45^\circ$ basis was measured for different mirror positions over a range of 8 mm with a step width of 0.2 mm, accumulating coincidence counts at each point for 30 seconds. All coincidences within the time window of $\tau = 256$ ns are counted and the results are shown in Fig. 3. Accidentals due to double pairs are subtracted and the data are corrected for power fluctuations in the pump. The statistical error bars are too small to be displayed. As expected for an unfiltered type-II SPDC source, the HOM dip shows a triangular shape [22].

The model that we use for the fit is based on the theory given in [23]. The coincidence rate R_{coin} is given in terms of the difference Δl between signal and idler paths, the average coincidence rate for large time differences R_{avg} and a parameter ζ with $\zeta = 4/(L|k'_s - k'_i|)$, that depends on the crystal length L and the k -vectors for signal and idler photons:

$$R_{\text{coin}}(\Delta l) = R_{\text{avg}} \left(1 - \wedge \left(\frac{\Delta l \zeta}{2c} \right) \right) \quad (1)$$

The function $\wedge(x)$ takes the value $\wedge(x) = 1 - |x|$ for $|x| < 1$ and $\wedge(x) = 0$ elsewhere. The theoretical prediction of the base-to-base width of the triangle $4c/\zeta = 2.03$ mm agrees well with the fitted value of 2.0 mm.

The drop of the coincidence rate for path differences larger than +2.5 mm is due to a change in coupling efficiency to the single-mode fibers, as the efficiency was optimized for translation stage positions close to the bottom of the dip. Therefore, data points over +2.5 mm were disregarded for the fit. The fit function displays a visibility defined by $V = (C_{\text{max}} - C_{\text{min}})/(C_{\text{max}} + C_{\text{min}})$ of 96% with subtraction of accidental counts and 83% without; the lowest point measured directly shows a visibility of 90%. To reduce the rate of accidental counts due to double pair generation even more, the HOM dip was also measured for a very low pump power of 12 μW . For this measurement the visibility for the lowest data point is 95% with subtraction of the accidentals and 90% for the raw data. This visibility clearly indicates the non-classical character of the down-converted photon pairs and their indistinguishability [24]. It should be noted that all our measurements were done without any spectral filtering.

5. Conclusion

In conclusion, we have demonstrated a high-brightness, highly efficient source of pairs of indistinguishable photons using a type-II OPO. Compared to other schemes it shows a higher degree of indistinguishability and a higher flux. Our setup achieves indistinguishability without any spectral or spatial filtering, which allows for the first time efficient coupling of high-quality photon pairs into single-mode fibers. A Hong-Ou-Mandel dip was measured with a visibility of over 90%. The source can easily be extended to provide beams of polarization-entangled photons by using an ordinary 50-50 beam splitter. The degenerate spectral mode with a linewidth of 7 MHz at 795 nm is estimated to contain 70 pairs/(s mW MHz), increasing the spectral

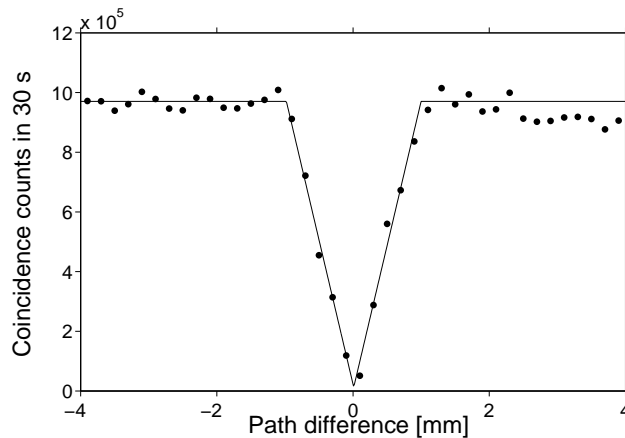


Fig. 3. Hong-Ou-Mandel Dip. Experimental data and triangular fit function.

brightness for pairs of indistinguishable photons by two orders of magnitude over the, to our knowledge, spectrally brightest comparable source reported so far. Depending on the application, filter cavities after the OPO could be used to isolate this degenerate mode or the unfiltered output could be directly applied on a frequency-selective system such as atoms. Since the spectral properties of this mode match perfectly the natural linewidth of the D_1 transition of atomic rubidium, the presented source provides photon pairs for efficient interaction with atomic systems. This is an essential requirement for the realization of an interface between light and matter on the single-photon level for quantum memories and quantum repeaters.

Acknowledgments

This work was supported by an ICFO-OCE Collaborative Research Program, by the Spanish Ministry of Science and Education under the FLUCMEM project (Ref. FIS2005-03394) and the Consolider-Ingenio 2010 Project “QOIT”, by NSERC, the Canadian Institute for Photonic Innovations, Ontario Centres of Excellence and QuantumWorks. F. W. and A. P. are supported by the Commission for Universities and Research of the Department of Innovation, Universities and Enterprises of the Catalan Government and the European Social Fund.